

QCD Evolution of the Sivers Function

S. M. Aybat,^{1,*} J. C. Collins,^{2,†} J. W. Qiu,^{3,4,‡} and T. C. Rogers^{5,6,§}

¹*Nikhef Theory Group, Science Park 105, 1098XG Amsterdam, The Netherlands*

²*Department of Physics, Pennsylvania State University, University Park, Pennsylvania 16802, USA*

³*Physics Department, Brookhaven National Laboratory, Upton New York 11973, USA*

⁴*C.N. Yang Institute for Theoretical Physics, Stony Brook University, Stony Brook New York 11794, USA*

⁵*Department of Physics and Astronomy, Vrije Universiteit Amsterdam, NL-1081 HV Amsterdam, The Netherlands*

⁶*C.N. Yang Institute for Theoretical Physics, Stony Brook University, Stony Brook NY 11794, USA*

(Dated: 22 February 2012)

We extend the Collins-Soper-Sterman (CSS) formalism to apply it to the spin-dependence governed by the Sivers function. We use it to give a correct numerical QCD evolution of existing fixed-scale fits of the Sivers function. With the aid of approximations useful for the nonperturbative region, we present the results as parametrizations of a Gaussian form in transverse-momentum space, rather than in the Fourier conjugate transverse coordinate space normally used in the CSS formalism. They are specifically valid at small transverse momentum. Since evolution has been applied, our results can be used to make predictions for Drell-Yan and semi-inclusive deep inelastic scattering at energies different from those where the original fits were made. Our evolved functions are of a form that they can be used in the same parton-model factorization formulas as used in the original fits, but now with a predicted scale dependence in the fit parameters. We also present a method by which our evolved functions can be corrected to allow for twist-3 contributions at large parton transverse momentum.

I. INTRODUCTION

High energy collisions with transversely polarized hadrons are ideal processes for extracting information about the structure of hadrons. The nonperturbative functions that enter into the corresponding factorization formulas are sensitive to novel aspects of QCD dynamics such as chiral symmetry breaking and the role of orbital angular momentum. (See e.g. [1] for some interesting recent discussions.) The Sivers function is an example which has received considerable attention in recent years, and will be the focus of this article, although many of the results and techniques are extendable to other interesting transverse-momentum dependent (TMD) functions. In loose terms, the Sivers function describes the transverse-momentum distribution of (unpolarized) partons inside a transversely polarized hadron (usually a proton). In semi-inclusive cross sections with a single transversely polarized target hadron, it leads to a characteristic $\sin(\phi - \phi_h)$ azimuthal modulation (ϕ and ϕ_h being the azimuthal angles of the transverse spin and the produced hadron, respectively). It is one of a collection of TMD parton distribution functions (PDFs) and fragmentation functions (FFs) that are actively being studied for the insight they can provide about hadron structure and the unique opportunities they provide for comparing theoretical descriptions with experimental results [2–6].

The Sivers effect was originally proposed more than

two decades ago in Ref. [7] as a mechanism for generating transverse single spin asymmetries (SSAs) in hadron-hadron collisions. Shortly afterward, it was argued in Ref. [8] on the basis of time-reversal (actually TP) invariance that the Sivers function vanishes. This result, if true, implies that the corresponding SSA in semi-inclusive deep inelastic scattering (SIDIS) is power-suppressed (i.e., it is of “higher twist”), leaving only the spin-dependent effects due to the Collins function in fragmentation. Thus, a contradiction arose when spectator model calculations [9] gave an explicit nonvanishing leading-twist SSA in SIDIS with the azimuthal dependence associated with the Sivers function. The situation was clarified in Ref. [10], where it was shown that the proof of vanishing of the Sivers function was incorrect in QCD, because it ignored the Wilson lines needed in the definitions of parton densities. Instead, the true consequence of TP invariance of QCD is that the Sivers function reverses sign between SIDIS and Drell-Yan (DY) processes. This is because future-pointing Wilson lines are needed in TMD functions like the Sivers function when used for SIDIS, but past-pointing Wilson lines are needed for the Drell-Yan process. At the level of the actual cross section, the sign-reversal for the Drell-Yan process was verified in model calculations in Ref. [11].

Certain other polarization or azimuthally dependent functions, such as the Boer-Mulders and the pretzelosity distributions [12, 13], also share this “T-odd” property of reversal of sign between SIDIS and Drell-Yan. Over the past decade, there has developed much work in the extraction, study, and formal theoretical description of these functions.

However, phenomenological fits of the Sivers function (and of related functions) have so far [14, 15] used only the simplest parton-model factorization formulas where

*Electronic address: maybat@nikhef.nl

†Electronic address: collins@phys.psu.edu

‡Electronic address: jqiu@bnl.gov

§Electronic address: rogers@insti.physics.sunysb.edu

the TMD parton densities and fragmentation functions do not evolve with the scale of the process, or use incorrect evolution formalisms. This is inadequate when they are to be applied to experiments at widely different energies. There is a good QCD formalism for applying TMD functions in a factorization framework, due to Collins, Soper and Sterman (CSS) [16, 17]. The CSS formalism gives a correct treatment of the region of low transverse momentum, which is where the Sivvers function analysis is used. However it has not been fully systematized for the case of the Sivvers function and other azimuthally-dependent functions, except in the work of Boer [18, 19] and Idilbi et al. [20], on which we comment below.

In this paper, we give a complete extension of the CSS method to processes that need the Sivvers function, using the methods recently given in Ref. [21]. It is straightforward to extend our results to the other azimuthally dependent PDFs and FFs (e.g., the Collins function and the Boer-Mulders function). We apply the formalism to give numerical results for the Sivvers function evolved from existing fits. The only extra nonperturbative information needed for the evolution is universal and is obtained from existing fits to the unpolarized Drell-Yan process. This extends the results given by two of us in Ref. [22] for the unpolarized case. Reference [15] attempts to include some effects of evolution by simply including the evolution from collinear factorization, but this is incorrect for TMD-factorization. It is also stated (Ref. [15], for example) that the true scale-evolution of the Sivvers function is unknown. One purpose of this article is to demonstrate that this is no longer true.

With the aid of an approximation useful for the non-perturbative region, we present the results as Gaussian transverse-momentum distributions with scale-dependent parameters. They are therefore as easy to use in simple parton-model-style calculations as the original fixed-scale fits [14, 15]. As the scale increases, the distributions broaden substantially in transverse momentum, and get diluted in size. It will be necessary to include perturbative twist-3 corrections to get more accurate values at the larger values of transverse momentum, and we present a scheme for how this should be done.

Boer [18, 19] has applied the CSS method to processes involving the Collins function. Idilbi et al. [20] have applied the CSS method to their definitions of various TMD distributions [23, 24] including the Sivvers function. Our treatment is substantially improved, to include a correct treatment of the nonperturbative region in CSS evolution applied to T-odd functions, to use a more modern

version of the CSS formalism, to apply it to the Sivvers function, and to obtain convenient numerical results for the Sivvers function.

Although it has recently become common for the word “resummation” to be used to indicate any CSS-like treatment, in our work we will maintain a firm distinction between resummation methodology and TMD-factorization. The term “resummation” is often used to indicate that one starts with conventional collinear factorization and resums logarithms of q_T/Q , which can in fact be done with the CSS methodology. The problem with this approach is that it is only valid when the underlying collinear factorization formula is valid, i.e., for the region where the transverse momentum q_T is both much less than the hard scale and much greater than hadronic binding energies $\sim \Lambda_{\text{QCD}}$. (See, in particular, the recent work of Ref. [25].) But to extend the calculations to transverse momenta comparable to Λ_{QCD} and to zero transverse momentum requires a complete TMD-factorization formalism, which we use here. This is particularly important because many SIDIS experiments such as HERMES and JLab are performed at kinematical scales where transverse momenta of order Λ_{QCD} are certainly important, and Q is not so large.

A number of difficulties are caused by the use of a pure resummation formalism rather than TMD factorization as the basis of calculations. For the present paper, one of the most significant is that a leading-power resummation formalism does not give the effects associated with the Sivvers function (and also those associated with the Boer-Mulders [26] function). But, provided that spin effects are treated correctly, the presence of these functions is automatic in TMD factorization, at leading power.

II. SETUP AND DEFINITIONS

In this section we give the factorization formula for SIDIS: $e + P(S) \rightarrow e + h + X$, and present the definitions of the TMD functions. We let P and S be the momentum and spin vector of the hadron target, and we let h label the detected hadron, of momentum p_h . With a single exchanged photon of momentum q , independent kinematic variables are: $Q = \sqrt{-q^2}$, $x = Q^2/2p \cdot q$, $z = P \cdot p_h/P \cdot q$, and the virtual photon’s transverse momentum \mathbf{q}_T (in a hadron frame where the measured hadrons have zero transverse momentum).

The TMD-factorization formula in the form derived by Collins [21] is:

$$W^{\mu\nu} = \sum_f |\mathcal{H}_f(Q; \mu)|^{\mu\nu} \int d^2\mathbf{k}_{1T} d^2\mathbf{k}_{2T} F_{f/P^\dagger}(x, \mathbf{k}_{1T}, S; \mu; \zeta_F) D_{h/f}(z, z\mathbf{k}_{2T}; \mu; \zeta_D) \delta^{(2)}(\mathbf{k}_{1T} + \mathbf{q}_T - \mathbf{k}_{2T}) + Y(Q, \mathbf{q}_T) + \mathcal{O}((\Lambda/Q)^a). \quad (1)$$

Here $F_{f/P^\dagger}(x, \mathbf{k}_{1T}, S)$ is the TMD PDF for an unpolarized quark of flavor f in a proton of polarization S , and $D_{h/f}(z, z\mathbf{k}_{2T})$ is the unpolarized fragmentation function. These factors contain nonkinematic parameters, μ , ζ_F , and ζ_D , whose definitions are given below. The hard-scattering factor $|\mathcal{H}^2|^{\mu\nu}$ is computed, with appropriate subtractions, from massless parton scattering in a photon frame where the photon and partons have zero transverse momentum — see [21, page 527] for its definition. The first line of the factorization formula is valid at low transverse momentum, and the Y term provides a correction for large transverse momentum in a form like that for ordinary collinear factorization. Although we will focus on SIDIS for this paper, the same general treatment applies also to DY scattering, up to the change in direction of the Wilson line in the definition of the TMD PDF. Note that the TMD-factorization piece, the first term in Eq. (1), is formulated specifically to deal with the small k_T behavior ($k_T \rightarrow 0$), while allowing for systematic corrections to the behavior as k_T grows larger than Λ_{QCD} .

The above formula is exactly like the parton-model formula for the same cross section except for the scale dependence of the PDF and fragmentation function and except for higher-order corrections in the hard scattering and Y -term. It differs from the older CSS formula by no longer needing an explicit soft factor. The factorization formula (1) is written for the case that the partons at the hard scattering are unpolarized. Parton polarization effects can be allowed for simply by inserting spin matrices for the incoming and outgoing partons of the hard scattering. This gives other terms, e.g., those with the Collins function in fragmentation, with their characteristic angular distributions in the cross section. It was recently suggested in Ref. [27] that it would be useful to analyze data for cross sections in transverse coordinate space b_T by taking various weighted integrals with Bessel functions. In that case, the b_T version of Eq. (1) is needed.

The parameter μ is a conventional renormalization scale, which we will choose to be in the $\overline{\text{MS}}$ scheme. It should be chosen to be of order Q so that the hard scattering has no large logarithms. The parameters ζ_F and ζ_D are related to the need to regulate rapidity divergences in the definitions of the TMDs. They are defined with the aid of an auxiliary rapidity parameter y_s , which has the function of separating forward and backward rapidity gluons. We use a hadron frame (in which the hadrons have zero transverse momentum), oriented so that $e^{y_P} \gg e^{y_{p_h}}$, and we let M_P and M_h be the masses of these hadrons. Then ζ_F and ζ_D are defined by

$$\zeta_F = M_P^2 x^2 e^{2(y_P - y_s)} \quad (2)$$

and

$$\zeta_D = (M_h^2/z^2) e^{2(y_s - y_h)}. \quad (3)$$

They obey $\sqrt{\zeta_F \zeta_D} = Q^2$ up to power-suppressed corrections, and have been normalized to correspond to CSS's definitions.

The definitions of gauge-invariant TMD functions are equipped with Wilson lines. A Wilson line (or gauge link) from a point x to ∞ along the direction of a four-vector n is defined as

$$W(\infty, x; n) = P \exp \left[-ig_0 \int_0^\infty ds \, n \cdot A_0^a(x + sn) t^a \right]. \quad (4)$$

Here, bare field operators and bare couplings are used and P is a path-ordering operation. The generator for the gauge group in the fundamental representation, with color index a , is denoted by t^a .

To define the parton densities, we use two lightlike directions that characterize the extreme forward and backward directions:

$$u_A = (1, 0, \mathbf{0}_T), \quad u_B = (0, 1, \mathbf{0}_T). \quad (5)$$

These correspond to the directions of P and p_h . Our coordinates for a 4-vector v are defined by

$$v = (v^+, v^-, v_T) \quad (6)$$

where,

$$v^\pm = (v^0 \pm v^z)/\sqrt{2}. \quad (7)$$

Now the most obvious definitions of PDFs use lightlike Wilson lines, which give rise to rapidity divergences [28]. Regulating the divergences can be done by using non-light-like Wilson lines. So we define vectors $n_A(y_A)$ and $n_B(y_B)$ with finite rapidities y_A and y_B :

$$n_A = (1, -e^{-2y_A}, \mathbf{0}_T), \quad n_B = (-e^{2y_B}, 1, \mathbf{0}_T). \quad (8)$$

The actual TMD PDF in Eq. (1) is defined as a limit of an unsubtracted TMD multiplied by certain unsubtracted soft functions. These are first defined in transverse coordinate space and then the final result will be Fourier transformed to transverse-momentum space. The unsubtracted TMD PDF is

$$\begin{aligned} \tilde{F}_{f/P^\dagger}^{\text{unsub}}(x, \mathbf{b}_T, S; \mu; y_P - y_B) \\ = \text{Tr}_C \text{Tr}_D \int \frac{dw^-}{2\pi} e^{-ixP^+ w^-} \langle P, S | \bar{\psi}_f(w/2) W(w/2, \infty, n_B(y_B))^\dagger \frac{\gamma^+}{2} W(-w/2, \infty, n_B(y_B)) \psi_f(-w/2) | P, S \rangle_c \end{aligned} \quad (9)$$

where $w^\mu = (0^+, w^-, \mathbf{b}_T)$, and we notate the functions with a tilde to indicate the use of transverse coordinate space. The subscript c indicates that only connected diagrams are included, and Tr_C and Tr_D represent color and Dirac traces respectively. The unsubtracted soft function is

$$\tilde{S}_{(0)}(\mathbf{b}_T; y_A, y_B) = \frac{1}{N_c} \langle 0 | W(\mathbf{b}_T/2, \infty; n_B)_{ca}^\dagger W(\mathbf{b}_T/2, \infty; n_A)_{ad} W(-\mathbf{b}_T/2, \infty; n_B)_{bc} W(-\mathbf{b}_T/2, \infty; n_A)_{db} | 0 \rangle. \quad (10)$$

In both of these functions, there should be inserted transverse gauge links at infinity. However, their effects cancel in the subtracted TMD PDF, when Feynman gauge is used, so we have not indicated the extra gauge links explicitly.

The full definition of the TMD PDF from [21] is

$$\tilde{F}_{f/P^\dagger}(x, \mathbf{b}_T, S; \mu, \zeta_F) = \tilde{F}_{f/P^\dagger}^{\text{unsub}}(x, \mathbf{b}_T, S; \mu; y_P - (-\infty)) \sqrt{\frac{\tilde{S}_{(0)}(\mathbf{b}_T; +\infty, y_s)}{\tilde{S}_{(0)}(\mathbf{b}_T; +\infty, -\infty) \tilde{S}_{(0)}(\mathbf{b}_T; y_s, -\infty)}} Z_F Z_2. \quad (11)$$

This involves limits: infinite rapidity on the Wilson lines indicated, infinite length for the Wilson lines, and then removal of the UV regulator (dimensional regularization). The factors $Z_F Z_2$ at the end of Eq. (11) are the field strength and TMD renormalization factors respectively. Notice that two of the soft factors have one of their rapidity arguments equal to the finite parameter y_s .

An exactly analogous definition applies to the fragmentation function (see Ref. [21] for the explicit definition). In our notation, capital letters will denote unintegrated quantities and lower case letters will denote quantities integrated over transverse momentum. Otherwise, we will stick as closely as possible to the Trento conventions [29].

The momentum-space TMD PDF is

$$F_{f/P^\dagger}(x, \mathbf{k}_T, S; \mu, \zeta_F) = \frac{1}{(2\pi)^2} \int d^2 \mathbf{b}_T e^{i\mathbf{k}_T \cdot \mathbf{b}_T} \tilde{F}_{f/P^\dagger}(x, \mathbf{b}_T, S; \mu, \zeta_F). \quad (12)$$

This has dependence on the azimuthal angle between \mathbf{k}_T and the transverse spin vector \mathbf{S}_T of the target hadron. (We normalize \mathbf{S}_T so that its maximum size is unity.) The TMD PDF is decomposed as usual into the unpolarized TMD PDF and a spin-dependent term:

$$F_{f/P^\dagger}(x, k_T, S; \mu, \zeta_F) = F_{f/P}(x, k_T; \mu, \zeta_F) - F_{1T}^{\perp f}(x, k_T; \mu, \zeta_F) \frac{\epsilon_{ij} k_T^i S_T^j}{M_p}, \quad (13)$$

with $F_{1T}^{\perp f}(x, k_T; \mu, \zeta_F)$ being the Sivers function.

III. EVOLUTION OF THE SIVERS FUNCTION

In this section we generalize CSS evolution from the unpolarized TMDs to the Sivers function. Similar methods apply to the other TMDs with azimuthal dependence.

The general CSS formalism works equally well for these functions [21]. But it involves Fourier transformations in two transverse dimensions, and for practical use it is convenient to perform the azimuthal integrals analytically and to write the transforms in terms of integrals over the sizes of the transverse variables. The treatment of the azimuthal integrals provided in Sec. III A closely parallels previous treatments in Refs. [20, 23] and recently in [27].

A. Coordinate Space Representation of Azimuthal Dependence

To analyze the evolution of the last term in Eq. (13) we extract the azimuth-dependent part by defining

$$\phi_{f/P}^i(x, \mathbf{k}_T; \mu, \zeta_F) \equiv \frac{k_T^i}{M_p} F_{1T}^{\perp f}(x, k_T; \mu, \zeta_F), \quad (14)$$

in terms of which the complete Sivers term is

$$F_{1T}^{\perp f}(x, k_T; \mu, \zeta_F) \frac{\epsilon_{ij} k_T^i S_T^j}{M_p} = \phi_{f/P}^i(x, \mathbf{k}_T; \mu, \zeta_F) \epsilon_{ij} S_T^j. \quad (15)$$

The Fourier transform of the Siverts function is

$$\begin{aligned}\tilde{F}_{1T}^{\perp f}(x, b_T; \mu, \zeta_F) &= \int d^2 \mathbf{k}_T e^{-i \mathbf{k}_T \cdot \mathbf{b}_T} F_{1T}^{\perp f}(x, k_T; \mu, \zeta_F) \\ &= 2\pi \int_0^\infty dk_T k_T J_0(k_T b_T) F_{1T}^{\perp f}(x, k_T; \mu, \zeta_F),\end{aligned}\quad (16)$$

and the Fourier transform of $\phi_{f/P}^i(x, \mathbf{k}_T; \mu, \zeta_F)$ is

$$\begin{aligned}\tilde{\phi}_{f/P}^i(x, \mathbf{b}_T; \mu, \zeta_F) &= \int d^2 \mathbf{k}_T e^{-i \mathbf{k}_T \cdot \mathbf{b}_T} \phi_{f/P}^i(x, \mathbf{k}_T; \mu, \zeta_F) \\ &= \int d^2 \mathbf{k}_T e^{-i \mathbf{k}_T \cdot \mathbf{b}_T} \frac{k_T^i}{M_P} F_{1T}^{\perp f}(x, k_T; \mu, \zeta_F) \\ &= \frac{1}{M_P} \int d^2 \mathbf{k}_T \frac{i \partial}{\partial b_{Ti}} e^{-i \mathbf{k}_T \cdot \mathbf{b}_T} F_{1T}^{\perp f}(x, k_T; \mu, \zeta_F).\end{aligned}\quad (17)$$

Using Eq. (16) gives

$$\tilde{\phi}_{f/P}^i(x, \mathbf{b}_T; \mu, \zeta_F) = i \frac{1}{M_P} \frac{b_T^i}{b_T} \tilde{F}_{1T}^{\prime \perp f}(x, b_T; \mu, \zeta_F), \quad (18)$$

where we have denoted the derivative of $\tilde{F}_{1T}^{\perp f}$ with re-

spect to the length of \mathbf{b}_T by

$$\tilde{F}_{1T}^{\prime \perp f}(x, b_T; \mu, \zeta_F) \equiv \frac{\partial \tilde{F}_{1T}^{\perp f}(x, b_T; \mu, \zeta_F)}{\partial b_T}. \quad (19)$$

As we will see shortly, it is this derivative \tilde{F}' and not the function \tilde{F} itself that gets used in the evolution equations and in the formula for the Siverts term in the actual transverse-momentum dependence in Eq. (13).

Taking an inverse Fourier transform of Eq. (18) allows $\phi_{f/P}^i(x, \mathbf{k}_T; \mu, \zeta_F)$ to be rewritten in terms of Eq. (19):

$$\begin{aligned}\phi_{f/P}^i(x, \mathbf{k}_T; \mu, \zeta_F) &= \frac{1}{(2\pi)^2} \int d^2 \mathbf{b}_T e^{i \mathbf{k}_T \cdot \mathbf{b}_T} \tilde{\phi}_{f/P}^i(x, \mathbf{b}_T; \mu, \zeta_F) \\ &= \frac{i}{(2\pi)^2 M_P} \int d^2 \mathbf{b}_T e^{i \mathbf{k}_T \cdot \mathbf{b}_T} \frac{b_T^i}{b_T} \tilde{F}_{1T}^{\prime \perp f}(x, b_T; \mu, \zeta_F).\end{aligned}\quad (20)$$

To further simplify this expression, and without loss of generality, we use a frame where \mathbf{k}_T is in the x direction so that $\frac{k_T^i}{k_T} = (1, 0)$ and $\frac{b_T^i}{b_T} = (\cos \theta, \sin \theta)$. Then,

$$\begin{aligned}\phi_{f/P}^i(x, \mathbf{k}_T; \mu, \zeta_F) &= \frac{i}{(2\pi)^2 M_P} \int_0^\infty db_T b_T \tilde{F}_{1T}^{\prime \perp f}(x, b_T; \mu, \zeta_F) \int_{-\pi}^\pi d\theta e^{i k_T b_T \cos \theta} (\cos \theta, \sin \theta) \\ &= \frac{1}{(2\pi)^2 M_P} \int_0^\infty db_T b_T \tilde{F}_{1T}^{\prime \perp f}(x, b_T; \mu, \zeta_F) \frac{\partial}{\partial (k_T b_T)} \int_{-\pi}^\pi d\theta e^{i k_T b_T \cos \theta} (1, 0) \\ &= \frac{k_T^i}{2\pi M_P k_T} \int_0^\infty db_T b_T \tilde{F}_{1T}^{\prime \perp f}(x, b_T; \mu, \zeta_F) \frac{\partial}{\partial (k_T b_T)} J_0(k_T b_T) \\ &= \frac{-k_T^i}{2\pi M_P k_T} \int_0^\infty db_T b_T J_1(k_T b_T) \tilde{F}_{1T}^{\prime \perp f}(x, b_T; \mu, \zeta_F).\end{aligned}\quad (21)$$

Then the complete Siverts term in Eq. (13) is

$$\phi_{f/P}^i(x, \mathbf{k}_T; \mu, \zeta_F) \epsilon_{ij} S_T^j = \frac{-k_T^i \epsilon_{ij} S_T^j}{2\pi M_P k_T} \int_0^\infty db_T b_T J_1(k_T b_T) \tilde{F}_{1T}^{\prime \perp f}(x, b_T; \mu, \zeta_F). \quad (22)$$

So, from Eq. (15) we express the momentum-space Siverts function in terms of \tilde{F}' :

$$F_{1T}^{\perp f}(x, k_T; \mu, \zeta_F) = \frac{-1}{2\pi k_T} \int_0^\infty db_T b_T J_1(k_T b_T) \tilde{F}_{1T}^{\prime \perp f}(x, b_T; \mu, \zeta_F). \quad (23)$$

whose inverse transform is

$$\tilde{F}_{1T}^{\prime \perp f}(x, b_T; \mu, \zeta_F) = -2\pi \int_0^\infty dk_T k_T^2 J_1(k_T b_T) F_{1T}^{\perp f}(x, k_T; \mu, \zeta_F). \quad (24)$$

Notice that the originally defined $\tilde{F}_{1T}^{\perp f}$ from Eq. (16) no longer appears. The b_T -dependent function $\tilde{F}_{1T}^{\prime \perp f}(x, b_T; \mu, \zeta_F)$ is closely analogous to the quantity $\tilde{f}_{1T}^{\perp(1)}$ that appears in Eqs. (16) and (20) of Ref. [27], and to $\partial_b^i q_T$ in Eq. (40) of Ref. [20], though the basic definition for the b_T -space TMD PDF in Eq. (11) is significantly different.

B. The Evolution Equations

The set of evolution equations comprises the Collins-Soper (CS) equation which gives evolution with respect

to ζ_F , and the RG equations which give evolution with

respect to μ . The CS equation for the TMD function defined in Eq. (11) is [21]

$$\frac{\partial \tilde{F}_{f/P^\uparrow}(x, \mathbf{b}_T, S; \mu, \zeta_F)}{\partial \ln \sqrt{\zeta_F}} = \tilde{K}(b_T; \mu) \tilde{F}_{f/P^\uparrow}(x, \mathbf{b}_T, S; \mu, \zeta_F), \quad (25)$$

where

$$\tilde{K}(b_T; \mu) = \frac{1}{2} \frac{\partial}{\partial y_s} \ln \left(\frac{\tilde{S}(b_T; y_s, -\infty)}{\tilde{S}(b_T; +\infty, y_s)} \right). \quad (26)$$

The RG equations are

$$\frac{d\tilde{K}(b_T; \mu)}{d \ln \mu} = -\gamma_K(g(\mu)) \quad (27)$$

and

$$\begin{aligned} \frac{d\tilde{F}_{f/P^\uparrow}(x, \mathbf{b}_T, S; \mu, \zeta_F)}{d \ln \mu} \\ = \gamma_F(g(\mu); \zeta_F/\mu^2) \tilde{F}_{f/P^\uparrow}(x, \mathbf{b}_T, S; \mu, \zeta_F). \end{aligned} \quad (28)$$

Similar equations apply to the fragmentation function.

It follows that the ζ_F dependence of γ_F is determined:

$$\frac{\partial \gamma_F(g(\mu); \zeta_F/\mu^2)}{\partial \ln \sqrt{\zeta_F}} = -\gamma_K(g(\mu)), \quad (29)$$

so that

$$\gamma_F(g(\mu); \zeta_F/\mu^2) = \gamma_F(g(\mu); 1) - \frac{1}{2} \gamma_K(g(\mu)) \ln \frac{\zeta_F}{\mu^2}. \quad (30)$$

These equations were used in Ref. [22] to calculate the evolution of the unpolarized TMDs. For the spin-dependent case, the Fourier transform of the second term in Eq. (13) obeys the same evolution equations, i.e., the equations apply to

$$\begin{aligned} \int d^2 \mathbf{k}_T e^{-i \mathbf{k}_T \cdot \mathbf{b}_T} F_{1T}^{\perp f}(x, k_T; \mu, \zeta_F) \frac{\epsilon_{ij} k_T^i S_T^j}{M_p} \\ = \tilde{\phi}_{f/P}^i(x, \mathbf{b}_T; \mu, \zeta_F) \epsilon_{ij} S_T^j. \end{aligned} \quad (31)$$

The CS equation for the spin-dependent part is therefore

$$\begin{aligned} \frac{\partial \tilde{\phi}_{f/P}^i(x, \mathbf{b}_T; \mu, \zeta_F) \epsilon_{ij} S_T^j}{\partial \ln \sqrt{\zeta_F}} \\ = \tilde{K}(b_T; \mu) \tilde{\phi}_{f/P}^i(x, \mathbf{b}_T; \mu, \zeta_F) \epsilon_{ij} S_T^j. \end{aligned} \quad (32)$$

Hence, Eq. (18) shows that the CS equation for $\tilde{F}_{1T}^{\perp f}(x, b_T; \mu, \zeta_F)$ is the same as for the unpolarized TMD PDF:

$$\frac{\partial \ln \tilde{F}_{1T}^{\perp f}(x, b_T; \mu, \zeta_F)}{\partial \ln \sqrt{\zeta_F}} = \tilde{K}(b_T; \mu). \quad (33)$$

Similarly, its RG equation is like Eq. (28):

$$\begin{aligned} \frac{d\tilde{F}_{1T}^{\perp f}(x, b_T; \mu, \zeta_F)}{d \ln \mu} \\ = \gamma_F(g(\mu); \zeta_F/\mu^2) \tilde{F}_{1T}^{\perp f}(x, b_T; \mu, \zeta_F). \end{aligned} \quad (34)$$

Note that in Eqs. (33) and (34) the same CS kernel $\tilde{K}(b_T; \mu)$ and anomalous dimension $\gamma_F(g(\mu); \zeta_F/\mu^2)$ appear as in the unpolarized case. This is because \tilde{K} and γ_F are properties of the operator defining the parton density, and this operator is the same for the ordinary unpolarized TMD PDF as for the Siverson function; both concern the number density of quarks in a hadron, with no polarization restriction on the quark.

It is important to emphasize that the evolution equations (25, 27, 28) are set up to be exactly correct for all b_T , and for all k_T . This includes the region where $b_T \rightarrow \infty$ (and hence $k_T \rightarrow 0$). Indeed, the first term on the right side of Eq. (1) (the TMD-factorization term) is designed to give an accurate pQCD treatment when $k_T \ll Q$, independently of the relative sizes of k_T and Λ_{QCD} .

C. Power laws for k_T and b_T dependence

As a guide to the qualitative behavior of the Siverson function, we summarize in this section the power laws for its dependence on transverse momentum and transverse position as obtained from simple model calculations. (For a detailed treatment of the power law behavior of other TMDs, see Ref. [30] and also recent discussions in Ref. [27].) In purely perturbative higher-order calculations, these get modified by logarithms, while use of a correct solution of the evolution equations can significantly modify the power laws [31]. Nevertheless, the power laws from elementary perturbative calculations form a useful standard of comparison.

First, we characterize the power law for an ordinary unpolarized TMD PDF by

$$F(x, k_T) \sim \frac{1}{k_T^2 + M^2}. \quad (35)$$

At large k_T , the falloff $1/k_T^2$ is the simple dimensional-analysis power, appropriate to a theory with a dimensionless coupling. The increase at low k_T is tamed by an infra-red cutoff M , which in QCD is nonperturbative. In b_T space, the large- k_T behavior Fourier transforms to

$$\tilde{F}(x, b_T) \sim \text{constant} \times \text{logarithms} \quad (\text{as } b_T \rightarrow 0). \quad (36)$$

At large b_T , the falloff of \tilde{F} should be at least rapid enough that the integral over all b_T is convergent, to give a finite value for $F(x, k_T)$ at $k_T = 0$. Normally an exponential or Gaussian falloff is assumed (which is controlled by nonperturbative effects in QCD).

As for the Siverson function, its contribution to the quark density, $F_{1T}^{\perp f}(x, k_T) \epsilon_{ij} k_T^i S_T^j / M_p$, has a kinematic zero at

$k_T = 0$. In addition, it is a chirality-violating quantity, and at large k_T , this requires a suppression by a factor of mass divided by k_T relative to the unpolarized density. So we characterize the result by

$$F_{1T}^{\perp f}(x, k_T) \frac{\epsilon_{ij} k_T^i S^j}{M_p} \sim \frac{k_T M}{(k_T^2 + M^2)^2}. \quad (37)$$

For the Siverts function itself, we therefore have

$$F_{1T}^{\perp f}(x, k_T) \sim \frac{M^2}{(k_T^2 + M^2)^2}. \quad (38)$$

This falloff is characterized as “twist-3.” In b_T space, the behavior of the Fourier transform of (38) at small b_T is

$$\tilde{F}_{1T}^{\perp f}(x, b_T) \sim \text{constant} + b_T^2 \times \text{logarithms}. \quad (39)$$

However, as we saw, it is the *derivative* of this quantity with respect to b_T that is actually used, for which the behavior is linear:

$$\tilde{F}_{1T}^{\perp f}(x, b_T) \sim b_T \times \text{logarithms}. \quad (40)$$

Although the actual equations for evolution are the same for the Siverts function as for the standard unpolarized TMD PDF, there are substantial differences in the way in which the evolution is reflected in the numerical values of these functions in transverse-momentum space. Because $\tilde{F}_{1T}^{\perp f}$ is approximately linear in b_T at small b_T and because the J_1 Bessel function instead of J_0 appears in Eq. (21), the Fourier transform for the Siverts function is sensitive to larger b_T values than the transform for the unpolarized TMD. This also implies that the evolution of Siverts is subject to more uncertainty from the nonperturbative large- b_T region than that of the unpolarized TMD.

D. Small- b_T expansion

For the unpolarized TMD PDF, an expansion for small b_T can be made in terms of the integrated PDFs. After Fourier transformation, this gives both the large- k_T behavior, and the normalization of the integral over the whole small k_T region.

The same idea continues to apply when we include the dependence of the TMD density on the target polarization. We can write

$$\tilde{F}(x, \mathbf{b}_T, S) = \sum_j \text{coefficient}_j \otimes \langle P, S | \text{operator}_j | P, S \rangle, \quad (41)$$

where the coefficients and operators are unaltered since they are properties of the TMD number-density operator. But the twist-2 operator on the right-hand side of (41) is the ordinary number-density operator used to define an integrated PDF, and its matrix element is independent of transverse spin. Thus the twist-2 operator, corresponding to a $1/k_T^2$ fall off at large k_T , provides no contribution to the Siverts function in Eq. (41). The leading large- k_T behavior of the Siverts function is the $1/k_T^3$ term associated with the twist-3 operators, the same operators that are used in the Qiu-Sterman formalism [32].

IV. OBTAINING EVOLVED SIVERS FUNCTIONS

In this section, we discuss the steps for obtaining the evolved Siverts function using already existing fits to the nonperturbative parts.

A. Solution in terms of fixed-scale Siverts function

Previous fits [14, 15] of the Siverts function used the parton-model formula for the hadronic tensor. We now show how these can be converted to use the correct QCD formula.

The parton-model version of TMD factorization amounts to applying the following approximations to the true QCD formula (1):

- (i) Replace the hard scattering by its lowest order.
- (ii) Neglect the Y term.
- (iii) Omit the evolution of the TMD PDFs.

If the renormalization scale μ is taken of order Q , higher-order corrections to the hard scattering are purely perturbative. One of the simplifications for TMD factorization is that these are just an overall factor, dependent on Q only through the running coupling $\alpha_S(Q)$. This factor is the same, independent of the hadron and the quark polarization, so it does not affect the ratio of the Siverts function to the ordinary TMD PDF.

The Y term only affects large transverse momentum (of order Q), whereas the data is dominantly at transverse momenta in the nonperturbative region. So the neglect of Y should be an adequate approximation with present data, and is easily corrected in the future, with the aid of fits for the Qiu-Sterman twist-3 function.

For a fixed value of Q , the TMD functions can be given fixed values of μ and ζ_F , $\mu = Q$ and $\zeta_F = Q^2$, and the QCD factorization formula is the same as the parton-model formula, up to an overall K -factor. This legitimizes the fixed-scale fits. But as can be seen from Fig. 1 below, evolution gives substantial changes in the TMD PDFs needed at higher Q . These are easily obtained, in their transverse-coordinate-space form, in terms of the parton-model fits at a fixed scale. We derive the necessary result starting from Eqs. (33), (34), and (30).

In these equations, the anomalous dimensions γ_F and γ_K are perturbatively calculable, but the function \tilde{K} at large values of b_T is nonperturbative. We follow Ref. [17] to separate the perturbative and nonperturbative parts of \tilde{K} . First, we define

$$\mathbf{b}_* = \frac{\mathbf{b}_T}{\sqrt{1 + b_T^2/b_{\max}^2}}, \quad \mu_b = \frac{C_1}{b_*}. \quad (42)$$

Here C_1 is a fixed numerical coefficient and b_{\max} is chosen to keep b_* in the perturbative region. In the fits to unpolarized Drell-Yan, the values chosen were

$b_{\max} = 0.5 \text{ GeV}^{-1}$ in [33], and $b_{\max} = 1.5 \text{ GeV}^{-1}$ in [34]. Next we write

$$\tilde{K}(b_T; \mu) = \tilde{K}(b_*; \mu_b) - \int_{\mu_b}^{\mu} \frac{d\mu'}{\mu'} \gamma_K(g(\mu')) - g_K(b_T). \quad (43)$$

The first two terms are perturbative and include all the evolution of \tilde{K} . The last term is nonperturbative but

scale independent. It represents the only nonperturbative information needed to evolve the Siverson function from the scale Q_0 where it was initially fit. But this function is process independent [21], so we can take its value from already existing fits to unpolarized Drell-Yan [33, 34] scattering at a variety of energies.

This gives the evolved function:

$$\begin{aligned} \tilde{F}'^{\perp f}_{1T}(x, b_T; \mu, \zeta_F) = \tilde{F}'^{\perp f}_{1T}(x, b_T; \mu_0, Q_0^2) \exp \left\{ \ln \frac{\sqrt{\zeta_F}}{Q_0} \tilde{K}(b_*; \mu_b) + \int_{\mu_0}^{\mu} \frac{d\mu'}{\mu'} \left[\gamma_F(g(\mu')); 1 \right] - \ln \frac{\sqrt{\zeta_F}}{\mu'} \gamma_K(g(\mu')) \right\} \\ + \int_{\mu_0}^{\mu_b} \frac{d\mu'}{\mu'} \ln \frac{\sqrt{\zeta_F}}{Q_0} \gamma_K(g(\mu')) - g_K(b_T) \ln \frac{\sqrt{\zeta_F}}{Q_0} \Big\}. \quad (44) \end{aligned}$$

We can set $\mu_0 = Q_0$ and then use $Q_0 = \sqrt{2.4} \text{ GeV}$, which is the appropriate scale for the fits in [14, 15], which used data from the HERMES experiment. For the prediction of data at a higher energy, one should set $\mu^2 = \zeta_F = Q^2$. The anomalous dimensions γ_F and γ_K are used in a region where perturbative calculations are appropriate.

The Siverson function in transverse-momentum space is then obtained from Eq. (44) by Fourier transformation, as in Eq. (23).

The one-loop values of the relevant perturbative quantities are listed in the Appendix.

The size of the Siverson asymmetry is also often parametrized by the function

$$\begin{aligned} F_{f/P^\uparrow}(x, \mathbf{k}_T; S, \mu, \zeta_F) - F_{f/P^\uparrow}(x, \mathbf{k}_T; -S, \mu, \zeta_F) \\ = \Delta^N F_{f/P^\uparrow}(x, k_T; \mu, \zeta_F) \frac{\epsilon_{ij} k_T^i S_T^j}{k_T}, \quad (45) \end{aligned}$$

where

$$\Delta^N F_{f/P^\uparrow}(x, k_T) = -\frac{2k_T}{M_p} F_{1T}^{\perp f}(x, k_T; \mu, \zeta_F). \quad (46)$$

Following the method used for the unpolarized TMD PDF — see Ref. [17, 21] and Eq. (31) of Ref. [22] — we write

$$\begin{aligned} \tilde{F}'^{\perp f}_{1T}(x, b_T; \mu, \zeta_F) = \sum_j \frac{M_p b_T}{2} \int_x^1 \frac{d\hat{x}_1 d\hat{x}_2}{\hat{x}_1 \hat{x}_2} \tilde{C}_{f/j}^{\text{Sivers}}(\hat{x}_1, \hat{x}_2, b_*; \mu_b^2, \mu_b, g(\mu_b)) T_{Fj/P}(\hat{x}_1, \hat{x}_2, \mu_b) \\ \times \exp \left\{ \ln \frac{\sqrt{\zeta_F}}{\mu_b} \tilde{K}(b_*; \mu_b) + \int_{\mu_b}^{\mu} \frac{d\mu'}{\mu'} \left[\gamma_F(g(\mu')); 1 \right] - \ln \frac{\sqrt{\zeta_F}}{\mu'} \gamma_K(g(\mu')) \right\} \times \exp \left\{ -g_{f/P}^{\text{Sivers}}(x, b_T) - g_K(b_T) \ln \frac{\sqrt{\zeta_F}}{Q_0} \right\}. \quad (47) \end{aligned}$$

The first line describes the matching to a collinear treatment relevant to small b_T . There, $\tilde{F}'^{\perp f}_{1T}(x, b_T; \mu, \zeta_F)$ is expressed as a coefficient function

As can be seen from Figs. 1 and 2 below, TMD functions broaden substantially as the scale increases. Thus larger values of transverse momentum become important, and correspondingly we need the \tilde{F} factor at small b_T .

B. Including the perturbative calculation of Siverson function at small- b_T

At low scales, the Siverson function is dominantly at low values of k_T , and correspondingly the range of b_T that matters concerns the larger values where both the starting value $\tilde{F}'^{\perp f}_{1T}(x, b_T; \mu_0, Q_0^2)$ and the evolution kernel $\tilde{K}(b_T; \mu)$ are in the nonperturbative region. After evolution to a sufficiently large scale, the broadening of the k_T distribution makes smaller values of b_T important, where there is perturbative information. For both this case and the treatment of the large- k_T tail of the Siverson function we can use the expansion (41) to write it in terms of the twist-3 Qiu-Sterman function.

$\tilde{C}_{f/j}(\hat{x}_1, \hat{x}_2, b_*; \mu_b^2, \mu_b, g(\mu_b))$ convoluted with a (twist-3) Qiu-Sterman function $T_{Fj/P}(\hat{x}_1, \hat{x}_2, \mu_b)$, where for the simplicity, we neglected the terms proportional to the

derivative of the twist-3 Qiu-Sterman function. On the second line, the first exponential comes from the perturbative part of the evolution of the Siverson function; the use of b_* and μ_b ensures that \tilde{C} , \tilde{K} , γ_F , and γ_K are in the perturbative region. The second exponential gives a correction to allow for nonperturbative behavior at larger b_T . In its exponent are both the nonperturbative term $g_K(b_T)$ for the evolution kernel, and an extra term $g_{f/P}^{\text{Sivers}}(x, b_T)$ for the Siverson function itself. These terms are both scale independent.¹

The coefficient \tilde{C} can be determined, for example, by performing a low-order perturbative calculation of the left-hand side of Eq. (47), of the Qiu-Sterman function, and of the first exponential, while ignoring the nonperturbative correction [25]. The normalization factor, $M_p b_T/2$, in Eq. (47) ensures that $T_F(\hat{x}_1, \hat{x}_2, \mu_b)$ has the standard normalization [25], and at zeroth order the contribution to the hard coefficient $\tilde{C}_{f/j}^{\text{Sivers}}(\hat{x}_1, \hat{x}_2, b_*, \mu_b^2, \mu_b, g(\mu_b))$ is

$$\tilde{C}_{f/j}^{\text{Sivers}, (0)}(\hat{x}_1, \hat{x}_2, b_*, \mu_b^2, \mu_b, g(\mu_b)) = \delta_{f,j} \delta(1 - x/\hat{x}_1) \delta(1 - x/\hat{x}_2), \quad (48)$$

which is similar to the zeroth order term in Eq. (A11) of Ref. [22] for the unpolarized case. (Recall that, since the Qiu-Sterman function $T_F(\hat{x}_1, \hat{x}_2, \mu_b)$ is universal, an extra minus sign is needed if we consider Drell-Yan instead of SIDIS.) The factor of b_T in the normalization is a reminder that it is the *derivative* of the Siverson function that we evolve in Eq. (47), not the Siverson function itself. Higher-order contributions to the coefficient function can be taken directly from work, such as Ref. [25], which treats smaller b_T within the Qiu-Sterman method. Calculations of the unpolarized coefficient functions to higher orders in the $\overline{\text{MS}}$ scheme have already been carried out in Ref. [21, 22].

The corresponding formula for the unpolarized TMD PDFs is very useful, since instead of the Qiu-Sterman function it uses the ordinary integrated PDFs, which are very well measured. In contrast, the phenomenology of the Qiu-Sterman function is less well known quantitatively, so there may be less of an advantage of using Eq. (47) instead of Eq. (44).

In the remaining sections, we will discuss the implementation of evolution, given some nonperturbative input functions, and provide specific evolved fits. Before continuing, however, we should emphasize that matters related to the fitting of the nonperturbative functions, including the choice of functional form for $g_K(b)$ and the matching procedure in Eq. (42), are unrelated to the validity of the TMD-factorization formalism itself. The TMD-factorization formalism automatically accom-

modates any refinements to knowledge about the non-perturbative physics. Indeed, a central aim of this article is to demonstrate the generality of the method. In our calculations below, we have chosen to consider fits to the nonperturbative functions that correspond to detailed studies of existing data. In addition to providing tools for phenomenology, our calculations illustrate how numerical values for the Siverson function corresponding to the definition in Eq. (11) can be obtained, once the non-perturbative functions are constrained by data. Thus, our use of TMD-factorization is closely analogous to what already exists for collinear factorization.

V. GAUSSIAN PARAMETRIZATIONS IN THE LOW- q_T REGION

In this section we explain the implementation of QCD evolution for the Siverson function with a Gaussian ansatz. Since the small- b_T region is twist-3, the tail of the (momentum-space) Siverson function (at large k_T) is power suppressed relative to the unpolarized TMD function. Furthermore, as illustrated in Ref. [22], a Gaussian parametrization provides a good description of the low transverse-momentum behavior, even up to transverse momenta of a few GeV. Therefore, we take as a starting point a detailed treatment of the twist-2 large- b_T behavior, leaving for future refinements an account of the matching of the small- b_T behavior to the twist-3 factorization formalism. That is, we use Eq. (44) rather than Eq. (47).

Even so, a full treatment that extends to small- b_T by including higher orders in $\tilde{C}_{f/j}(\hat{x}_1, \hat{x}_2, b_*, \mu_b^2, \mu_b, g(\mu_b))$ will be crucial in the long run for a complete understanding of the evolved Siverson function over the full range of b_T . This is especially important to keep in mind when dealing with weighted integrals of the Siverson function where the effect of the large transverse-momentum tail becomes magnified. We intend to pursue this in future refinements of the TMD approach.

At the initial fitting scale, we drop the explicit scale dependence:

$$\tilde{F}_{1T,0}'^{\perp}(x, b_T) = \tilde{F}_{1T}'^{\perp f}(x, b_T; \mu_0, Q_0^2). \quad (49)$$

To match previous fits [14, 15], we approximate the input function by a Gaussian

$$\tilde{F}_{1T,0}'^{\perp f}(x, b_T) = -\frac{\langle k_T^2 \rangle_0 f_{1T}^{\perp}(x) b_T}{2} \exp[-\langle k_T^2 \rangle_0 b_T^2/4], \quad (50)$$

which corresponds also to a Gaussian ansatz for the momentum-space distribution:

$$F_{1T,0}^{\perp f}(x, k_T) = \frac{f_{1T}^{\perp f}(x)}{\langle k_T^2 \rangle_0^f \pi} \exp[-k_T^2/\langle k_T^2 \rangle_0^f]. \quad (51)$$

The parameter $\langle k_T^2 \rangle_0^f$ is the width of the Siverson function for a quark of flavor f at the scale where the Gaussian fit is performed. Comparing with Eq. (47), we

¹ Note that our sign convention on $g_{f/P}^{\text{Sivers}}(x, b_T)$ and $g_K(b_T)$ is opposite of Ref. [22].

see that $g_{f/P}^{\text{Sivers}}(x, b_T) = \langle k_T^2 \rangle_0^f b_T^2 / 4$. The fits performed in [14, 15] are for quite low scales ($Q^2 = 2.4 \text{ GeV}^2$ for HERMES data). We therefore assume that the Sivers function is dominated by the nonperturbative large- b_T region, in which case a Gaussian description, with a negligible tail effect, makes sense. The first moment of the input momentum-space Sivers function obeys the usual relation:

$$f_{1T,0}^{\perp(1)}(x) = \int d^2 \mathbf{k}_T \frac{k_T^2}{2M_P^2} F_{1T,0}^{\perp}(x, k_T) = \frac{\langle k_T^2 \rangle_0}{2M_P^2} f_{1T}^{\perp}(x). \quad (52)$$

We again remind the reader that for our calculations, we are assuming a Sivers function for SIDIS and that a sign flip is necessary to go to DY.

With $g_K(b_T)$ already known from previous fits to high energy Drell-Yan data [33–35], all that is now needed in order to obtain evolved Gaussian fits are $\langle k_T^2 \rangle_0^f$ and $f_{1T}^{\perp f}(x)$. These will come from previously obtained fixed-scale Gaussian fits. In the next section, we will provide two examples and illustrate the effect of evolution for two of the sets of Gaussian fits available in the literature.

The function $g_K(b_T)$ is the only nonperturbative input that is necessary apart from these initial fits. We have also adopted the standard Gaussian ansatz for $g_K(b_T)$, writing $g_K(b_T) = g_2 b_T^2 / 2$. Fits like those of Refs. [33–35] provide numerical values for g_2 . In the Brock-Landry-Nadolsky-Yuan fits [33] a value of $g_2 = 0.68 \text{ GeV}^2$ is found. This corresponds to a value for b_{max} of 0.5 GeV^{-1} , and is what we will use in the fits of the next section.

VI. SPECIFIC FITS

In this section we provide examples of evolved fits, obtained by following the steps of Sec. V with specific fits for the input distributions. We remind the reader that our numerical calculations correspond to the Sivers function of SIDIS, and that they acquire an overall minus sign in the Drell-Yan process.

A. Bochum Fits

The fits of Ref. [14] use a Gaussian to describe the HERMES measurements [36] which were performed with an average Q^2 of 2.41 GeV^2 . We refer to these as the *Bochum fits*. The function corresponding to $f_{1T}^{\perp f}(x)$ in Eq. (51) is

$$\left[f_{1T}^{\perp \text{up/down}}(x) \right]_{\text{Bochum}} = \pm \frac{2M_P^2}{\langle k_T^2 \rangle_0} A x^{b-1} (1-x)^5. \quad (53)$$

The fit parameters are

$$A = 0.17, \quad b = 0.66.$$

In the Bochum fits, the parameter corresponding to $\langle k_T^2 \rangle_0^f$ in Eq. (51) is assumed to be independent of flavor and

lies between 0.10 and 0.32 GeV^2 . We take

$$\langle k_T^2 \rangle_0^f \text{Bochum} = \langle k_T^2 \rangle_0 \text{Bochum} = 0.2 \text{ GeV}^2, \quad (54)$$

which corresponds to the “best fit” scenario of Ref. [14].

Samples of the result of using the Bochum fits in Eq. (44) to evolve to different Q are shown in the upper panel of Fig. 1. The curves are shown for $Q = \sqrt{2.4, 5, 91.19} \text{ GeV}$ since these are also the values already used to illustrate the evolution of the unpolarized distribution functions in Ref. [22].

B. Torino Fits

Next we consider the fits of Ref. [15] which incorporated data from both HERMES [37] and COMPASS [38, 39]. Again, the scale for the initial distributions is $Q^2 = 2.4 \text{ GeV}^2$. We refer to these as the *Torino fits*. The function corresponding to $f_{1T}^{\perp f}(x)$ in Eq. (51) is

$$\left[f_{1T}^{\perp f}(x) \right]_{\text{Torino}} = -\frac{M_p \sqrt{2e}}{M_1 \langle k_T^2 \rangle} \mathcal{N}_f(x) f_f(x) \langle k_T^2 \rangle_0, \quad (55)$$

where

$$\mathcal{N}_f(x) \equiv N_f x^{\alpha_f} (1-x)^{\beta_f} \frac{(\alpha_f + \beta_f)^{(\alpha_f + \beta_f)}}{\alpha_f^{\alpha_f} \beta_f^{\beta_f}}, \quad (56)$$

and $f_f(x)$ is the unpolarized parton distribution function for quarks of flavor f . The fit parameters N_f , α_f , β_f are

$$N_u = 0.35, \quad \alpha_u = 0.73, \quad \beta_u = 3.46, \quad (57)$$

$$N_d = 0.90, \quad \alpha_d = 1.08, \quad \beta_d = 3.46, \quad (58)$$

and $M_1^2 = 0.34 \text{ GeV}^2$, $\langle k_T^2 \rangle = 0.25 \text{ GeV}^2$. The Gaussian slope parameter of the initial input distribution in the Torino fits is again flavor-independent and is

$$\langle k_T^2 \rangle_0^f \text{Torino} = \langle k_T^2 \rangle_0 \text{Torino} = \frac{M_1^2 \langle k_T^2 \rangle}{M_1^2 + \langle k_T^2 \rangle}. \quad (59)$$

For the integrated PDFs in Eq. (55), we have used the lowest-order MSTW parametrizations [40–43]. Samples of the evolved Torino fits are shown in the lower panel of Fig. 1.

Note that there is over a factor of 2 difference between the Torino and the Bochum fits, and this gives a rough indication of the uncertainty involved in current treatments. A discussion of the difference in the two methods can be found in Ref. [44].

We do hope for future improvements of the fits. A very recent parametrization of the nonperturbative input was presented in Ref. [45]. The results are similar to the Torino fits above, but utilize a relation to generalized parton distributions, and allow for a connection to a quantification of parton angular momentum. Moreover, model calculations, such as in Refs. [46, 47], and

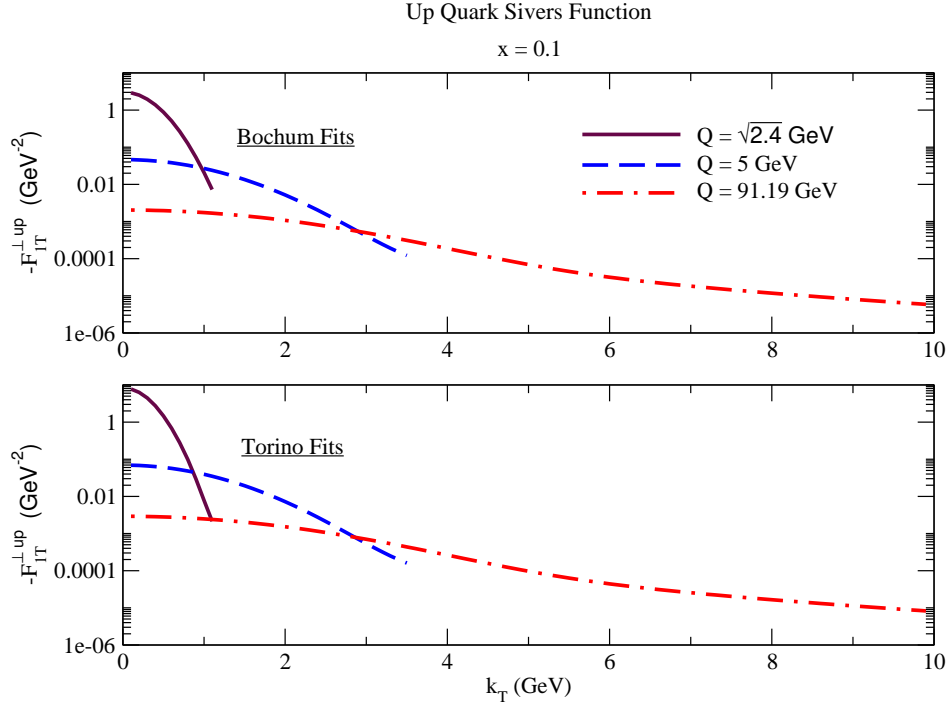


FIG. 1: (Color online.) The (negative of the) up quark Sivers function at $x = 0.1$ evolved from $Q = \sqrt{2.4}$ GeV (solid maroon) to $Q = 5$ GeV (dashed blue) and $Q = 91.19$ GeV (dot-dashed red). The upper plot is found by evolving the Gaussian fits of the Bochum group [14] and the lower plot is found by evolving the Gaussian fits of the Torino group [15]. In the case of the Bochum fits, the down quark Sivers function is just the negative of the up quark one. For the Torino fits, the down quark Sivers function is obtained by multiplying the up quark Sivers function by -1.35 . These functions acquire an overall reversal of sign if used in Drell-Yan.

lattice QCD calculations [48] can aid in providing meaningful parametrizations of the nonperturbative input over the whole of phase space and open up interesting questions regarding the matching of purely nonperturbative descriptions of the Sivers function to pQCD.

C. Evolved Gaussian Parametrizations

Figure 1 suggests that, apart from the tail at large k_T , the Sivers function continues to be well described by a Gaussian shape, even after evolution to large Q . To describe the evolution of a purely Gaussian parametrization, with the x and k_T dependence factorized, requires only a specification of the scale dependence of the Gaussian parameters. This saves having to directly calculate Eq. (44), and its transformation to momentum space, separately for each value of Q and x . Because of the general convenience of working with Gaussian functions, we have obtained Gaussian fits for a range of Q starting at $Q = \sqrt{2.4}$ GeV for the Bochum and Torino fits up to $Q = 90$ GeV. The fits are obtained using the Wolfram MATHEMATICA 7 FINDFIT routine, and examples are shown as the dashed curves in Fig. 2. A table of the resulting values for the Gaussian parameters is shown in Table I. (Fortran, C++, and Wolfram MATHEMATICA 7 code that produce evolved Gaussian fits is available

at [49].)

In Fig. 2, we illustrate the quality of the Gaussian fits to the Sivers function at intermediate and large Q ($Q = 5$ GeV and 91.19 GeV, respectively). In practice, the Sivers effect is often probed via observables like Eq. (52), so we have plotted the integrand, $-2\pi k_T^3 F_{1T}^{\perp up}(x, k_T; \mu, Q)$. Note that, after the evolution to large Q , the $-2\pi k_T^3 F_{1T}^{\perp up}(x, k_T; \mu, Q)$ acquires a very broad tail for both the Bochum and Torino fits. The tail falls off slowly; for $Q = 91.19$ GeV, the ratio of the value of the Bochum fit at $k_T = 10$ GeV to the value at $k_T = 5$ GeV is about 0.65. This is roughly consistent with the $1/k_T$ fall-off at large k_T that is expected from the power counting arguments in Sec. III C. The last two columns in Table I show the values of k_T where the ratio of the Gaussian fits to the original Sivers functions is 0.8. That is, above $k_{T,max}^{\text{Torino}}$ (GeV) the Gaussian fits to the evolved Torino Sivers function drop to less than 0.8 of the original evolved Sivers function and similarly for $k_{T,max}^{\text{Bochum}}$.

That the description at small k_T remains Gaussian is not entirely surprising given that the input we use for the nonperturbative evolution is Gaussian ($g_K(b_T) \propto b^2$). However, it should be emphasized that the perturbative contribution to evolution results in a substantial modification of the shape and normalization of the TMD PDF,

TABLE I: Table of evolved Gaussian parameters, obtained by fitting Gaussians to the evolved Bochum and Torino fixed-scale fits. The fits are for $x\Delta^N F_{f/P^\dagger}(x, k_T; \mu, \zeta_F)$ and are related to $F_{1T}^{\perp f}(x, k_T; \mu, \zeta_F)$ via Eq. (46). The parameters are listed for the up quark distributions at $x = 0.1$; the Siverson function at different values of x can be found by multiplying by the appropriate ratios obtained from Eqs. (53, 55). The Gaussian slope parameter b^{fit} is the same for the up and down quarks. The normalization parameters $a_{\text{up}}^{\text{fit}}$ are related to the down quark normalizations by $a_{\text{down}}^{\text{Bochum}} = -a_{\text{up}}^{\text{Bochum}}$ and $a_{\text{down}}^{\text{Torino}} \approx -1.35a_{\text{up}}^{\text{Torino}}$. The last two columns, $k_{T,\text{max}}^{\text{Bochum}}$ and $k_{T,\text{max}}^{\text{Torino}}$, are the values of k_T above which the Gaussian fits drop to less than a ratio of 0.8 of the Siverson functions calculated directly from Eq. (44).

$x\Delta^N F_{f/P^\dagger}^{\text{fit}}(x = 0.1, k_T) = a_f^{\text{fit}} k_T e^{-b^{\text{fit}} k_T^2}$						
Q (GeV)	b^{Bochum} (GeV ⁻²)	b^{Torino} (GeV ⁻²)	$a_{\text{up}}^{\text{Bochum}}$ (GeV ⁻³)	$a_{\text{up}}^{\text{Torino}}$ (GeV ⁻³)	$k_{T,\text{max}}^{\text{Bochum}}$ (GeV)	$k_{T,\text{max}}^{\text{Torino}}$ (GeV)
$\sqrt{2.4}$	4.9999	6.9382	6.5570×10^{-1}	1.7763×10^0
2.0	1.8251	2.0329	9.5506×10^{-2}	1.6661×10^{-1}
2.5	1.1726	1.2552	4.1658×10^{-2}	6.7105×10^{-2}	2.36	2.29
3.0	0.9067	0.9555	2.5716×10^{-2}	4.0138×10^{-2}	2.56	2.50
3.5	0.7604	0.7945	1.8430×10^{-2}	2.8276×10^{-2}	2.70	2.65
4.0	0.6668	0.6929	1.4329×10^{-2}	2.1745×10^{-2}	2.80	2.76
4.5	0.6013	0.6225	1.1718×10^{-2}	1.7649×10^{-2}	2.89	2.85
5.0	0.5526	0.5705	9.9179×10^{-3}	1.4854×10^{-2}	2.96	2.92
10.0	0.3562	0.3637	3.9881×10^{-3}	5.8409×10^{-3}	3.39	3.36
15.0	0.2941	0.2992	2.5477×10^{-3}	3.7049×10^{-3}	3.56	3.54
20.0	0.2612	0.2653	1.8893×10^{-3}	2.7372×10^{-3}	3.67	3.65
25.0	0.2400	0.2435	1.5090×10^{-3}	2.1810×10^{-3}	3.75	3.73
30.0	0.2249	0.2280	1.2602×10^{-3}	1.8182×10^{-3}	3.81	3.79
35.0	0.2135	0.2163	1.0841×10^{-3}	1.5621×10^{-3}	3.86	3.84
40.0	0.2044	0.2070	9.5257×10^{-4}	1.3712×10^{-3}	3.90	3.88
45.0	0.1969	0.1993	8.5046×10^{-4}	1.2232×10^{-3}	3.94	3.92
50.0	0.1907	0.1929	7.6878×10^{-4}	1.1049×10^{-3}	3.97	3.95
55.0	0.1853	0.1874	7.0188×10^{-4}	1.0081×10^{-3}	3.99	3.98
60.0	0.1806	0.1826	6.4604×10^{-4}	9.2744×10^{-4}	4.02	4.00
65.0	0.1765	0.1784	5.9868×10^{-4}	8.5906×10^{-4}	4.04	4.02
70.0	0.1728	0.1747	5.5800×10^{-4}	8.0035×10^{-4}	4.06	4.04
75.0	0.1695	0.1713	5.2267×10^{-4}	7.4937×10^{-4}	4.08	4.06
80.0	0.1665	0.1683	4.9164×10^{-4}	7.0467×10^{-4}	4.10	4.08
85.0	0.1638	0.1655	4.6421×10^{-4}	6.6514×10^{-4}	4.11	4.09
90.0	0.1613	0.1629	4.3976×10^{-4}	6.2993×10^{-4}	4.13	4.11

even at low k_T . Therefore, Table I is *not* the result of simply Fourier transforming the nonperturbative contribution to Eq. (44). Rather, to get the right TMD PDF, even when using a Gaussian approximation for low k_T , the full pQCD evolution must be included. We find that difference between the fitted Gaussian and the result obtained by naively Fourier transforming the nonperturbative part of the evolution is similar to what was found for the unpolarized TMD PDF (see Fig. 2 of Ref. [22]).

The presence of the tail illustrates the danger in evaluating moment integrals like Eq. (52) without a careful account of the large- k_T behavior. For $Q = 91.19$ GeV, there is more than 40% suppression in the integral of the curves in Fig. 2 from 0 to 10 GeV when the Gaussian fit is used rather than the fit including the tail. (Note that in principle the integral should be extended to order Q .) For the $Q = 5$ GeV curves, integrated up to 5 GeV, the

corresponding suppression is only about 9%.

By contrast, at low- k_T the Gaussian functions, shown as the dashed curves in Fig. 2, provide excellent approximations to the evolved Siverson function. This suggests that the evolved Gaussian approximation is especially suited to low- Q /low- k_T studies. A sample of evolved Gaussian fits for lower Q is shown in Fig. 3.

VII. DISCUSSION AND CONCLUSIONS

Many of the recent phenomenological efforts related to the study of transverse polarization effects in TMDs have assumed a lowest-order, generalized parton-model (GPM) picture [50] and work within a rather narrow range of energy scales. However, the full power of factorization theorems lies in their ability to make predictions

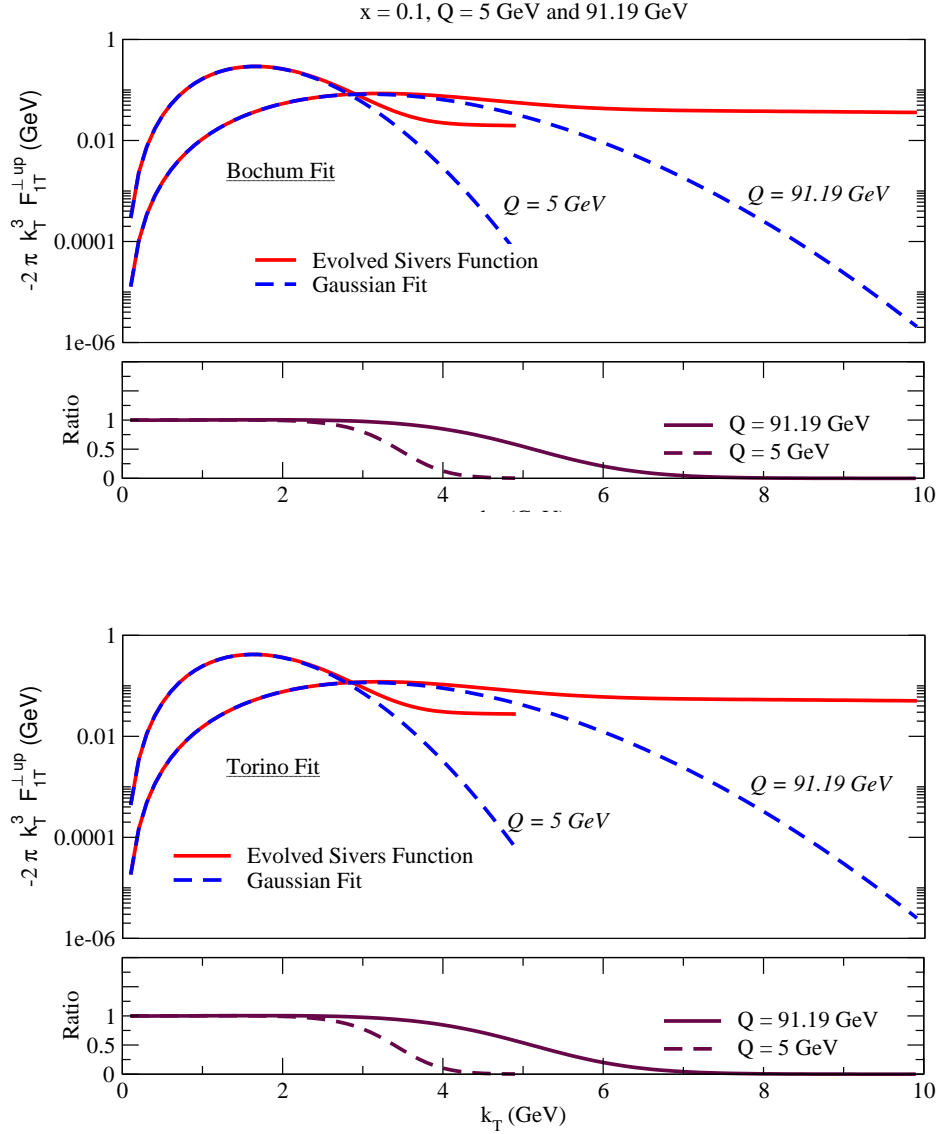


FIG. 2: (Color online.) The up quark Sivvers function at $Q = 5$ GeV and $Q = 91.19$ GeV (solid curves) and the corresponding Gaussian fit for the low- k_T region (dashed curves). Note that the function plotted is the Sivvers function multiplied by $-2\pi k_T^3$. The upper panel is obtained by evolving the Gaussian fits of the Bochum group [14] and lower panel is obtained by evolving the Gaussian fits of the Torino group [15]. Below each plot, the ratio between a Gaussian fit and the evolved function including the tail is also shown.

for a variety of processes over a wide range of energy scales. In this article, we have explained the steps for implementing evolution for polarization dependent TMD PDFs, specifically illustrated with the Sivvers function. The basic method is the CSS formalism [16, 17, 31], with the specific formulation of the TMD-factorization formalism given recently in Ref. [21]. An advantage of the most up-to-date TMD-factorization formula is that it is written in a form closely analogous to the GPM (see Eq. (1)), with explicit definitions for the individual TMDs. Therefore, existing treatments that rely on a GPM framework need only to replace the unevolved TMDs with the evolved ones. An important aspect of our approach is that it relies on a genuine, complete TMD-

factorization formalism, to be contrasted with the resummation methodology that has often been relied on in the past to treat many aspects of TMD physics. That is, the TMD-factorization formalism provides, from the outset, a consistent treatment of factorization for the full range of k_T (or, equivalently, the full range of b_T in coordinate space).

Fortunately, many of the results obtained from the treatment of unpolarized TMDs can be carried over directly to the polarization dependent case, including the calculation of the anomalous dimensions γ_F , γ_D and γ_K , and the CS evolution kernel K , in both its calculable perturbative part and its nonperturbative part $g_K(b_T)$ that is known from fits to unpolarized Drell-Yan. An impor-

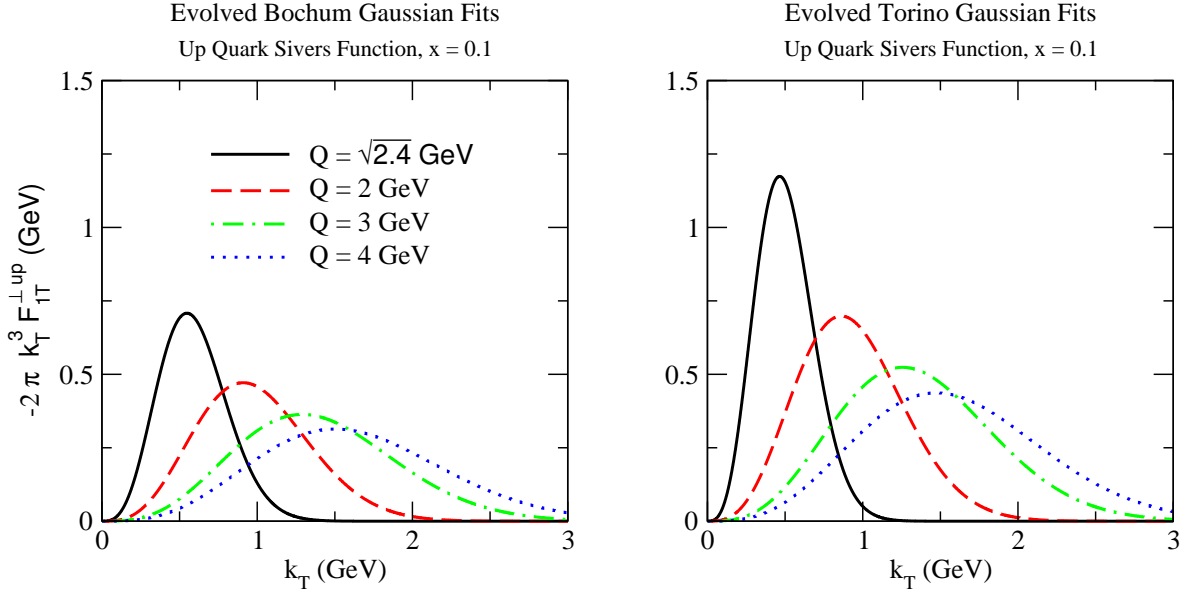


FIG. 3: (Color online.) The evolving Gaussian parameters for $-2\pi k_T^3 F_{1T}^{\perp up}(x, k_T; \mu, Q)$ for a range of Q obtained from the Torino and Bochum fits. Table I lists the Gaussian parameters for a selection of Q .

tant difference from the unpolarized case is in the matching at large- k_T . In the unpolarized case, the TMD PDF (or FF) matches to a twist-2 collinear factorization treatment at large k_T , whereas the Sivvers function matches to a twist-3 collinear factorization treatment related to the Qiu-Sterman formalism, as in Eq. (47). Thus, the treatment provided in this article unifies several different aspects of TMD physics.

It is worth commenting on the often repeated statement (see, e.g., Ref. [51]) that calculations in covariant gauges are impractical or inconvenient, and that working in light-cone gauge is therefore preferred. In our work, we find that the opposite is true. Namely, the calculation of the perturbative parts (at least to order α_s) follows clear-cut steps in Feynman gauge, while the derivation of TMD-factorization theorems is much more direct in Feynman gauge than in light-cone gauge. (Indeed, we are not aware of the existence of a detailed light-cone gauge derivation of TMD factorization.) Moreover, once the calculation of the perturbative parts has been performed in Feynman gauge, a generalized parton-model interpretation follows directly from the TMD-factorization formula in Eq. (1). For these reasons, we advocate continuing to work in Feynman gauge for both calculations and derivations.

We have implemented the evolution explicitly using as input the already known γ_F , γ_D and γ_K (supplied for easy reference in the Appendix, previous fixed-scale Gaussian fits of the Sivvers function at low- Q [14, 15], and previous fits of the CSS formalism to DY [33]. For the explicit calculations in the present article, we have focused only on the low- k_T region where we need not be concerned with the treatment of the Qiu-Sterman formalism at large k_T , and the approximations of Sec. V make sense.

The resulting evolved momentum-space Sivvers functions are shown in Fig. 1. Comparing with Fig. 1 of Ref. [22] for the evolution of the unpolarized TMD PDF, one sees even more suppression as Q is increased than in the unpolarized case. Also note that a significant perturbative tail is generated at large Q as shown in Fig. 2. We reemphasize that this should be kept in mind when evaluating integrals like Eq. (52).

Gaussian parametrizations are particularly convenient for doing explicit calculations. Therefore, we have tested the quality of Gaussian fits after evolution to large Q and find that the Gaussian function provides an excellent approximation to the Sivvers function at small k_T , even for $Q \approx 90.0$ GeV. We have made these fits available, as well as code for generating evolved TMDs at a website maintained by two of us (Aybat and Rogers) [49].

Much work remains to be done in the effort to connect a full QCD treatment of TMDs with phenomenology. An explicit implementation of the matching to the twist-3 Qiu-Sterman formalism is still needed, and will be particularly important for a correct treatment of k_T -weighted observables in which the extra k_T factors enhance the contribution from the large k_T region. The recent work of Ref. [25] may help. Moreover, as new data become available for both polarized and unpolarized cross sections, it will be useful to construct new fits that include evolution from the beginning. Finally, explicit calculations, analogous to the ones presented here, need to be applied to the other TMDs like the Boer-Mulders and Collins functions.

At large Q , the shape of the distribution is especially sensitive to the value of b_{\max} , g_2 and the functional form of $g_K(b_T)$. Reference [34], for example, finds that a larger value of b_{\max} is preferred, along with a corresponding

change in g_2 . Furthermore, Refs. [52, 53] find advantages to using a different functional form, $\sim b^{2/3}$ rather than $\sim b^2$, for $g_K(b_T)$. This should be taken into account in future improvements to the fits. The particular set of parameters used in the calculations in the present article were chosen both because of their simplicity and because they correspond to the current state-of-the-art of global fits to the unpolarized Drell-Yan cross section.

In the future, model calculations (see, e.g., [54] and references therein for an overview) can be potentially helpful for fixing nonperturbative input. Certain models also lead to nonperturbative input distributions that deviate from the Gaussian ansatz. Conversely, incorporating evolution into model calculations can help establish the scale appropriate to the model.

Theoretical uncertainties in the TMD fits, both for unpolarized and polarized TMDs, can be reduced by including higher-order results for the anomalous dimensions and the CSS kernel K (in the perturbative region). Fortunately, as we have discussed in this paper, these anomalous dimensions and the kernel K are the same for unpolarized TMDs and the Sivers function. Therefore by calculating them at next-to-next-to-leading order in pQCD, we can reduce the theoretical uncertainties for both unpolarized and polarized TMDs at the same time.

The ultimate goal is to obtain sets of TMD PDFs and FFs that can be used in a way that is closely analogous to what already exists for processes that use collinear factorization. Namely, we would like to obtain a set of TMD fits based on precise TMD definitions such that they can be reliably used to make predictions.

Acknowledgments

M. Aybat and T. Rogers acknowledge support from the research program of the “Stichting voor Fundamenteel

Onderzoek der Materie (FOM),” which is financially supported by the “Nederlandse Organisatie voor Wetenschappelijk Onderzoek (NWO).” M. Aybat also acknowledges support from the FP7 EU-programme Hadron-Physics2 (Contract No. 2866403). T. Rogers was also supported in part by the National Science Foundation, Grant No. PHY-0969739. J. C. Collins and J. W. Qiu were supported by the U.S. Department of Energy under Grant No. DE-FG02-90ER-40577 and Contract No. DE-AC02-98CH10886, respectively. M. Aybat and T. Rogers thank Christine Aidala, Aurore Courtoy, Bryan Field, and Alexei Prokudin for useful discussions.

APPENDIX: ANOMALOUS DIMENSIONS ETC.

Here we list the $\overline{\text{MS}}$ -scheme anomalous dimensions [21] that were used in, for example, Eqs. (44) and (47):

$$\gamma_F(\mu; \zeta_F/\mu^2) = \alpha_s \frac{C_F}{\pi} \left(\frac{3}{2} - \ln \left(\frac{\zeta_F}{\mu^2} \right) \right) + \mathcal{O}(\alpha_s^2). \quad (60)$$

At order α_s , the quark TMD FF anomalous dimension is the same as for the TMD PDF. The CS kernel up to order α_s in \mathbf{b}_T space is

$$\tilde{K}(\mu, b_T) = -\frac{\alpha_s C_F}{\pi} [\ln(\mu^2 b_T^2) - \ln 4 + 2\gamma_E] + \mathcal{O}(\alpha_s^2). \quad (61)$$

The anomalous dimension of \tilde{K} is up to order α_s ,

$$\gamma_K(\mu) = 2\frac{\alpha_s C_F}{\pi} + \mathcal{O}(\alpha_s^2). \quad (62)$$

-
- [1] D. Sivers (2011), 1109.2521.
 - [2] D. Boer, M. Diehl, R. Milner, R. Venugopalan, W. Vogelsang, et al. (2011), 1108.1713.
 - [3] *PHENIX decadal plan, October 2010, available at <http://www.phenix.bnl.gov/phenix/www/docs/decadal12010/phenixdecadal12010.pdf>*
 - [4] *STAR decadal plan, December 2010, available at http://www.bnl.gov/npp/docs/star_decadal_plan_final12010.pdf*
 - [5] Z. Lu, B.-Q. Ma, and J. Zhu (2011), 1108.4974.
 - [6] Z.-B. Kang, J.-W. Qiu, W. Vogelsang, and F. Yuan, Phys.Rev. **D83**, 094001 (2011), 1103.1591.
 - [7] D. W. Sivers, Phys. Rev. **D41**, 83 (1990).
 - [8] J. C. Collins, Nucl. Phys. **B396**, 161 (1993), hep-ph/9208213.
 - [9] S. J. Brodsky, D. S. Hwang, and I. Schmidt, Phys. Lett. **B530**, 99 (2002), hep-ph/0201296.
 - [10] J. C. Collins, Phys. Lett. **B536**, 43 (2002), hep-ph/0204004.
 - [11] S. J. Brodsky, D. S. Hwang, and I. Schmidt, Nucl. Phys. **B642**, 344 (2002), hep-ph/0206259.
 - [12] D. Boer and P. J. Mulders, Phys. Rev. **D57**, 5780 (1998), hep-ph/9711485.
 - [13] H. Avakian, A. V. Efremov, P. Schweitzer, and F. Yuan, Phys. Rev. **D78**, 114024 (2008), 0805.3355.
 - [14] J. C. Collins, Phys. Rev. **D73**, 014021 (2006), hep-ph/0509076.
 - [15] M. A. J. M. Afselmimo et al., Eur. Phys. J. **A39**, 89 (2009), 0805.2677.
 - [16] J. C. Collins and D. E. Soper, Nucl. Phys. **B194**, 445 (1982).
 - [17] J. C. Collins, D. E. Soper, and G. F. Sterman, Nucl. Phys. **B250**, 199 (1985).
 - [18] D. Boer, Nucl. Phys. **B603**, 195 (2001), hep-ph/0102071.
 - [19] D. Boer, Nucl. Phys. **B806**, 23 (2009), 0804.2408.
 - [20] A. Idilbi, X.-d. Ji, J.-P. Ma, and F. Yuan, Phys.Rev. **D70**, 074021 (2004), hep-ph/0406302.
 - [21] J. C. Collins, *Foundations of Perturbative QCD* (Cambridge University Press, Cambridge, 2011).
 - [22] S. M. Aybat and T. C. Rogers, Phys. Rev. **D83**, 114042

- (2011), 1101.5057.
- [23] X.-d. Ji, J.-P. Ma, and F. Yuan, Phys.Lett. **B597**, 299 (2004), hep-ph/0405085.
 - [24] X.-d. Ji, J.-p. Ma, and F. Yuan, Phys.Rev. **D71**, 034005 (2005), hep-ph/0404183.
 - [25] Z.-B. Kang, B.-W. Xiao, and F. Yuan, Phys.Rev.Lett. **107**, 152002 (2011), 1106.0266.
 - [26] D. Boer and P. Mulders, Phys.Rev. **D57**, 5780 (1998), hep-ph/9711485.
 - [27] D. Boer, L. Gamberg, B. Musch, and A. Prokudin (2011), 1107.5294.
 - [28] J. Collins, PoS **LC2008**, 028 (2008), 0808.2665.
 - [29] A. Bacchetta, U. D'Alesio, M. Diehl, and C. A. Miller, Phys. Rev. **D70**, 117504 (2004), hep-ph/0410050.
 - [30] A. Bacchetta, D. Boer, M. Diehl, and P. J. Mulders, JHEP **08**, 023 (2008), 0803.0227.
 - [31] J. C. Collins and D. E. Soper, Nucl. Phys. **B197**, 446 (1982).
 - [32] J. W. Qiu and G. F. Sterman, Phys.Rev. **D59**, 014004 (1998), hep-ph/9806356.
 - [33] F. Landry, R. Brock, P. M. Nadolsky, and C. P. Yuan, Phys. Rev. **D67**, 073016 (2003), hep-ph/0212159.
 - [34] A. V. Konychev and P. M. Nadolsky, Phys. Lett. **B633**, 710 (2006), hep-ph/0506225.
 - [35] G. A. Ladinsky and C. P. Yuan, Phys. Rev. **D50**, R4239 (1994), hep-ph/9311341.
 - [36] A. Airapetian et al. (HERMES), Phys. Rev. Lett. **94**, 012002 (2005), hep-ex/0408013.
 - [37] M. Dieffenthaler (HERMES) (2007), 0706.2242.
 - [38] A. Martin (COMPASS), Czech. J. Phys. **56**, F33 (2006), hep-ex/0702002.
 - [39] M. Alekseev et al. (COMPASS), Phys. Lett. **B673**, 127 (2009), 0802.2160.
 - [40] A. D. Martin, W. J. Stirling, R. S. Thorne, and G. Watt, Eur. Phys. J. **C63**, 189 (2009), 0901.0002.
 - [41] A. Martin, W. Stirling, R. Thorne, and G. Watt, Eur.Phys.J. **C64**, 653 (2009), 0905.3531.
 - [42] A. Martin, W. Stirling, R. Thorne, and G. Watt, Eur.Phys.J. **C70**, 51 (2010), 1007.2624.
 - [43] <http://projects.hepforge.org/mstwpdf/>.
 - [44] M. Anselmino et al. (2005), hep-ph/0511017.
 - [45] A. Bacchetta and M. Radici, Phys.Rev.Lett. **107**, 212001 (2011), 1107.5755.
 - [46] A. Courtoy, S. Scopetta, and V. Vento, Phys.Rev. **D79**, 074001 (2009), 0811.1191.
 - [47] A. Courtoy, F. Fratini, S. Scopetta, and V. Vento, Phys.Rev. **D78**, 034002 (2008), 0801.4347.
 - [48] B. U. Musch, P. Hagler, J. W. Negele, and A. Schafer, Phys.Rev. **D83**, 094507 (2011), 1011.1213.
 - [49] <http://projects.hepforge.org/tmd/>.
 - [50] U. D'Alesio and F. Murgia, Prog. Part. Nucl. Phys. **61**, 394 (2008), 0712.4328.
 - [51] I. Cherednikov and N. Stefanis, Int. J. Mod. Phys. Conf. Ser. **4**, 135 (2011), 1108.0811.
 - [52] J. W. Qiu and X.-f. Zhang, Phys.Rev. **D63**, 114011 (2001), hep-ph/0012348.
 - [53] E. L. Berger and J. W. Qiu, Phys.Rev. **D67**, 034026 (2003), hep-ph/0210135.
 - [54] H. Avakian, A. Efremov, P. Schweitzer, O. Teryaev, F. Yuan, et al., Mod.Phys.Lett. **A24**, 2995 (2009), 0910.3181.